ISSN: 3068-1774
Research Article

Journal of Material Sciences & Applied Engineering

The Development of Radiation Shielding Materials Involves Incorporating Lanthanum Oxide Dopants into Glass

Kaewjaeng, S[1]*, Ornketphon O[1] & Kaewkhao J [2,3]

[1]Department of Radiologic Technology, Faculty of Associated Medical Sciences, Chiang Mai University, Chiang Mai 50200, Thailand
[2]Physics Program, Faculty of Science and Technology, Nakhon Pathom Rajabhat University, Nakhon Pathom, 73000, Thailand
[3]Center of Excellence in Glass Technology and Materials Science (CEGM), Nakhon Pathom Rajabhat University, Nakhon Pathom, 73000, Thailand

***Corresponding author:** Siriprapa Kaewjaeng, Department of Radiologic Technology, Faculty of Associated Medical Sciences, Chiang Mai University, Chiang Mai 50200, Thailand.

Submitted: 17 September 2025 **Accepted:** 23 September 2025 **Published:** 29 September 2025

https://doi.org/10.63620/MKJMSAE.2025.

Citation: *Kaewjaeng, S., Ornketphon, O., & Kaewkhao, J. (2025). The Development of Radiation Shielding Materials Involves Incorporating Lanthanum Oxide Dopants into Glass. J of Mat Sci Apl Eng, 4(5), 01-09.*

Abstract

The glass formula (60-x) P2O5: 15Na2O: 5ZnO: 10Al2O3: 10CaO: xLa2O3 where x is 0, 5, 10, 15 and 20 mol%, is produced by using the melt quenching technique for photon shielding applications. The glasses were investigated for their physical, transmission, x-ray and gamma-ray shielding properties. The results discovered an increase in density with higher concentrations of La3+ions. The transmission spectra of the glass show higher transparency compared to x-ray windows. In relative studies of gamma-ray properties between experimental and theoretical data, the mass attenuation coefficients (MAC), effective atomic number (Zeff), and effective electron density (Neff) increased with the rising of La3+ ions. Conversely, the half-value layer (HVL) decreased, indicating an improvement in the radiation shielding material efficiency. In x-ray applications, the HVL decreased with an increase in La3+ ions content. The HVL value at a 20 mol% concentration of La3+ions is higher than standard materials at 120 kVp. The glass systems doped with La3+ ions could be potential candidates for x-ray and gamma-ray glass shielding in future applications.

Keywords: X-ray; Radiation; Shielding; Diagnostic; Ten Value Layer.

Introduction

Radiation shielding is a critical aspect of various fields, including nuclear energy, agriculture, space exploration and medical applications, where exposure to ionizing radiation posed significant health risk [1-5]. Effect radiation shielding significantly reduces the risk of radiation exposure for occupational worker, support staff, public, and surrounding population. Traditional radiation shielding equipment is continuously developed to increase safe alternatives for radiation protection, replacing lead (Pb) and offering cost-effective options. This includes considerations for shielding efficiency, resistance to chemical corrosion, and durability chemicals with high atomic number, such as lanthanum oxide (La2O3) most used in serving as a component in nuclear reactor systems, chemical industries, improved refractive index, excellent radiation attenuation, optical glass, and lenses. Therefore, La2O3 which makes it an ideal candidate for enhancing the shielding effectiveness of glass.

The materials that are widely chosen as a component for radiation shielding nowadays are glass. This is due to its good transparency, temperature resistance, and its ability melted or reshaped without altering its composition. Phosphate oxide (P2O5) glass is an option for shaping and use as a glass former due to its high transparency and low melting point [6-9].The addition aluminum oxide (Al2O3) and sodium oxide(Na2O) has been reported to reduce the melting point, thermal stability, low thermal expansion and enhance the strength of glass [10-12].In the context of zinc oxide (ZnO) being used to enhancing structure in glass formula, chemical durability, and providing good optical transparency in ultraviolet (UV) range it is useful in certain optical application. Calcium oxide (CaO) enhances the chemical resistance of the glass, increase mechanical strength, influences melting temperature and affects optical properties.

This research focuses on the formulation of a novel glass composite, represented by the formula (60-x) P2O5: 15Na2O:

5ZnO: 10Al2O3: 10CaO: xLa2O3 where x is 0, 5, 10, 15 and 20 mol%, respectively. Through a focus on x-ray, including the context of linear attenuation coefficient (μ), mass attenuation coefficient (MAC), half value layer (HVL), ten value layer (TVL), mean free path (MFP) and gamma-ray radiation shielding, this research involved calcution on XCOM programs. The details include mass attenuation coefficient (MAC), effective atomic number (Zeff) and effective electron density (Neff) on XCOM programs. There is potential to develop this glass sample into a radiation shielding material that could serve as a substitute for lead in the future.

Materials and Method

Glass Preparation

Lead-free radiation shielding materials are advantageous for human health, environmental, particularly for manufacturer process, due to their toxicity. In this research focused on lanthanum doped glasses as a potential alternative shielding materials in glass samples system in the formula (60-x) P2O5: 15Na2O: 5ZnO: 10AlF3: 10CaO: xLa2O3 where x is 0, 5, 10, 15 and 20 mol%, components, blend the components in the desired ratios. Next, mixture to high temperatures, typically around 1200°C, to melt and fuse the components together. After this, the glass is annealed by heating it to approximately 500°C and then gradually cooling it to enable structural alignment. This annealing procedure helps relieve internal stresses and enhances the glass durability. Once the glass is prepared, it will be cut and refined into shapes measuring 1 x 1.5 x 0.3 cm^3 to serve as control variables for characterization various properties.

Physical Properties

The weight of prepared glass samples was determined in both air and xylene using a high-precision 4-digi microbalance (A&D, HR-200). Applying Archimedes' principle, the density (ρ) was estimated according to the following equation [13].

Where Wa, is the weight in air, Wb is the weight in xylene and ρ_b is the density of xylene (ρ_b = 0.863 g/cm3).
The molar volume (Vm) was calculated from densities; it is equal to molecular weight (M) divided by density (ρ), expressed by the formula.

X-ray Radiation Shielding Characterization

The X-ray shielding characterization were measured using X-ray opeating the in the upper diagnostic energy range with a tungsten (W) target in X-ray tube, Shimadzu model RAD Speed Pro operated within the diagnostic X-ray energy range trypically employed in high frequency medical applicatios between 50-120 kVp technique. The radiation exposure was set at 100 mA and exposure time set at 0.2 sec (20 mAs). The radiation energies were recorded by using solid state detector model Accu-gold. The distance between the X-ray source and the detector was set at 50 cm during the measurements. To minimize backscattered radiation, the detector was positioned approximately 15 cm above the table. System energy calibration was performed to validate the radiation attenuation and transmission measurement tecchnique.

The x-ray radiation shielding characterization of (60-x)P2O5: 15Na2O: 5ZnO: 10Al2O3: 10CaO: xLa2O3 where x is 0, 5, 10, 15 and 20 mol% glass samples. The X-ray shielding analsis involves the determining key parameters such as the linear attenuation coefficient (LAC), the mass attenuation coefficient (MAC), half-value layer (HVL), ten-value layer (TVL), and mean free path (MFP), to assess the materials effectiveness in attenuating X-ray radiation. The data are crucial for understanding radiation shielding effectiveness. The X-ray radiation shielding, specifically in terms of the half-value layer (HVL), for glass samples with varying compositions of La2O3, is compared with standard radiation shielding materials, including commercial windows, brick, concrete, commercial lead glass (X-ray windows), concrete (NCRP No.49) and x-ray windows (NCRP No.49) [14].

The linear attenuation coefficient (LAC) is a fractional decrease in radiation fractional decrrese in radiation intensity per unit of thickness of materials. It is influenced by several parameters, and the study of these parameters can help optimize the design of X-ray shielding materials are the total probability of radiation interaction with matter was calculated using the appropriate attenuation coefficient derived from theoretical models, in equation.

$$I = I_0 e^{-m}$$

Where I am the intensity of the attenuated beam, I0 is the initial intensity, t (cm) is the thickness of the shielding material.

The half-value layer (HVL) is defined as the thickness of a materials required to attenuate the X-ray intensity by one-half (about 50%) its original values, and defined by the following equation.

$$x_{1/2} = \frac{0.693}{\mu}$$

Gamma Radiation Shielding Characterization

This work focused on heavy ion transport code system XCOM program is a computer program and database developed by the National Institute of Standards and Technology (NIST) to calculated photon interaction cross section for chemical composition in context of partial interaction, mass attenuation coefficient (MAC) to explained the possibility of partial interaction with in materials and calculated about effective atomic number (Zeff) and electron density (Neff). Zeff parameter is the average effect of all electrons in an atom on the behavior of gamma ray as they pass through a substance. It is a crucial parameter in interaction with ionizing radiation and can be calculated in formula; [15-23].

$$Z_{eff} = \frac{\sigma_{t,a}}{\sigma_{t,e}}$$

The total atomic cross-section (σt,a) can be determined from the mass attenuation coefficient by multiplying it with the material density;

$$\sigma_{t,a} = \frac{\mu_m}{N_A \sum_i^n \left(\frac{W_i}{A_i}\right)}$$

Where N_A represents the Avogadro's constant, Ai is the element of atomic weight of element i.Moreover, the total electronic cross-section (σt,el) for the element can be calculated using the formula;

$$\sigma_{t,e} = \frac{1}{N_A}\sum_{i}^{n}\frac{f_i A_i}{Z_i}(\mu_m)_i$$

where fi is the atomic fraction of element i, is calculated relative to the total number of atoms, whrer Zi represnets the atomic number of respective element.

The electron density (N_{eff}) is the number of electrons per unit volume in a materials that can interact with photon energy, and it can be calculated in the following form

$$N_{eff} = \frac{\mu_m}{\sigma_{t,e}}$$

Transmission Properties

The transmission properties of the glass samples, commercial window and x-ray window (lead glass) each with an equal thickness of about 3 mm. Data were collected at room temperature with the use of Variance Cary 50 spectrophotometer across UV-VIS-NIR regions.

Results and Discussions

Physical Properties

The density and molar volume of glass samples were measured are conducted in air and in xylene using A&D HR-200 4 digital sensitive microbalances, calculated in Archimedies's method. The density values increase from 2.655 to 2.873 g per cm3, respectively, for various concentration of La2O3 content in the glass samples. The glass samples exhibit an increasing trend in molar volume, stating from 43.045 to 55.150 cm3 per mol respectively. The molar volume of glass samples increased with addition of the chemical modifier La2O3, suggesting structural expansion within the glass matrix, are indicate in Fig. 1.

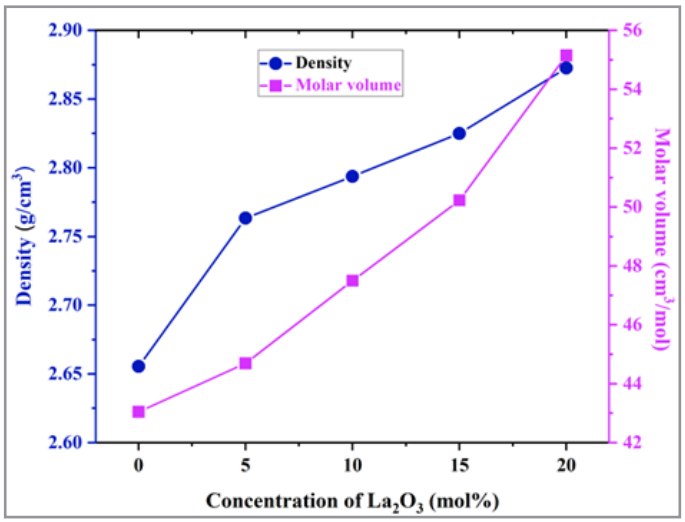

Figure 1: The Density and Molar Volume of Glass Samples

Transmission Properties

This study, the glass samples with the highest dopant concentrations (20% mol of La2O3) was selected to compare its optical transmission spectra with the standard reference material such as commercial window and x-ray windows. It has been observed that their transmission spectra are similar in the visible regions. The transmission spectra are indicated in Fig. 2.

The comparing the optical transmittance of glass samples with conventionally transparent materials, it is evident that these glasses not only offer efficient radiation shielding, also strong potential for future development as multifunctional shielding apploication.

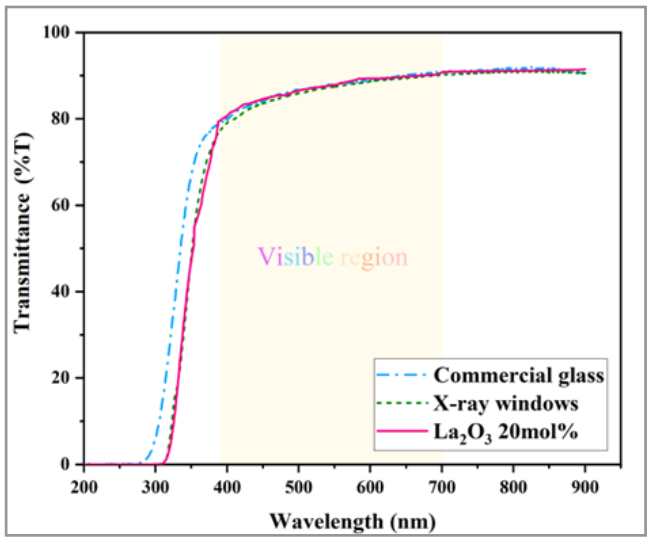

Figure 2: The Transmission Spectra of Glass Samples

X-ray Radiation Shielding

The X-ray radiation shielding properties are studies across varying parameters, specifically at energies levels commonly used in diagnostic radiology energy from low energies X-ray suitable for imaging thinner body parts, to high energy X-ray required for penetrating thicker anatomical regions. The study aims to determine key radiation parameters includes with linear attenuation coefficient (LAC), half-value layer (HVL), tenth value layer (TVL), and mean free path (MFP). To ensure the radiation shielding efficiency of the developed materials, its shielding performance was evaluated and against standard radiation shielding materials. This assessment was conducted to verify the feasibility of utilizing the researched material as a potential lead-free (Pb free) alternative for radiation shielding applications. The radiation shielding parameter data descripts below;

Linear Attenuation Coefficient (m)

The linear attenuation coefficient (LAC) of glass samples is depicted in Fig. 3 The results indicate that linear attenuation coefficient increases as the x-ray energies of glass samples increase.

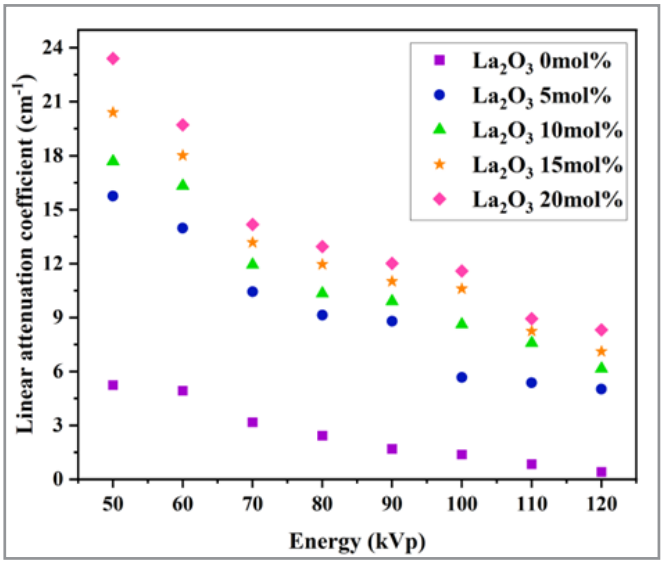

Figure 3: The LAC of Glass Samples

Ten Value Layers (TVL)

The tenth value layer (TVL) of glass sample decreased with increasing concentration of La3+ ions. This suggest that the addition of La3+ ions is making the glass effective at attenuating or absorbing radiation, as illustrated in the results indicate in Fig. 4.

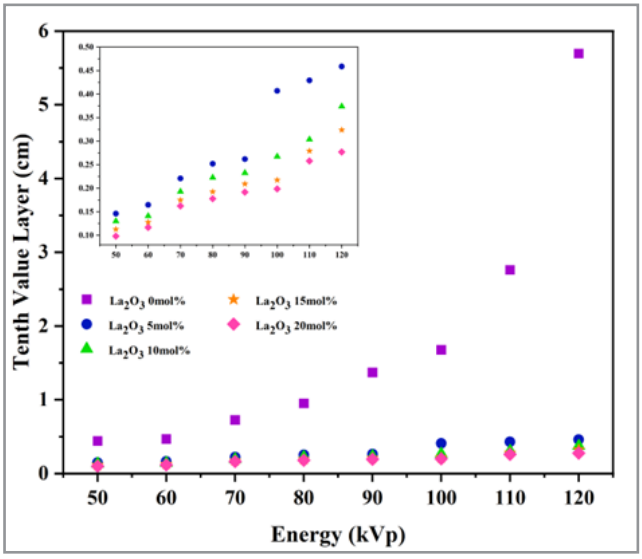

Figure 4: The TVL of La2O3 in the Glass Samples

The mean free path (MFP), determining the involves measuring or estimating the number density of particles and the collision cross-section in a particular medium, as illustrated in the results indicate in Fig. 5.

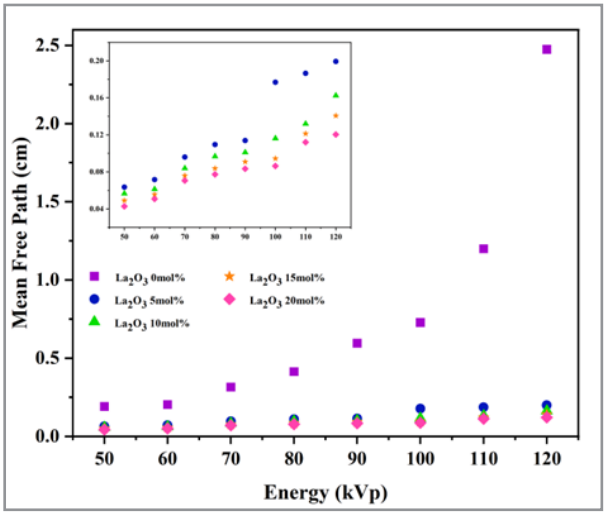

Figure 5: The MFP of La2O3 in the Glass Samples

Half-Value Layer (HVL)

The half-value layer (HVL) is a measure that reduces the radiation intensity of the primary beam more than 50%. The HVL were calculated using the equation depicted in Fig. 6.

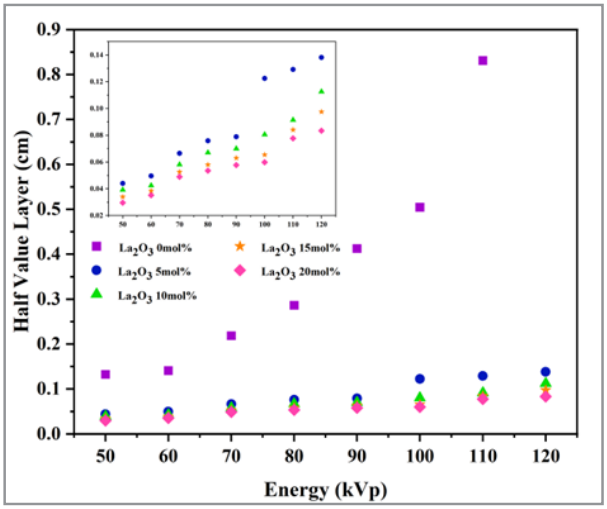

Figure 6: The HVL of Glass Samples.

The HVL of glass samples at each concentration using high kVp technique (120 kVp) are compared with standard materials, including commercial windows, brick, concrete, lead, x-ray windows, as depicted in Fig. 7.

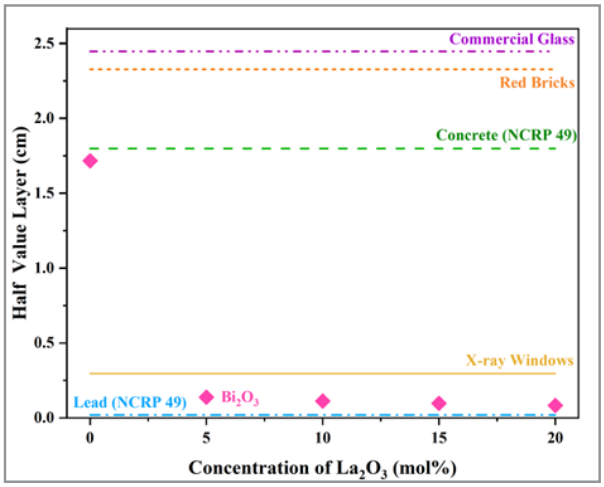

Figure 7: The HVL of Glass Samples Compared with Standard Materials.

Gamma ray Radiation Shielding

The comparative study of gamma-ray shielding energy from 0.15 to 15 MeV was conducted using XCOM programs, with focus on MAC, Zeff and Neff values. The MAC of glass samples is depicted in Fig. 8.

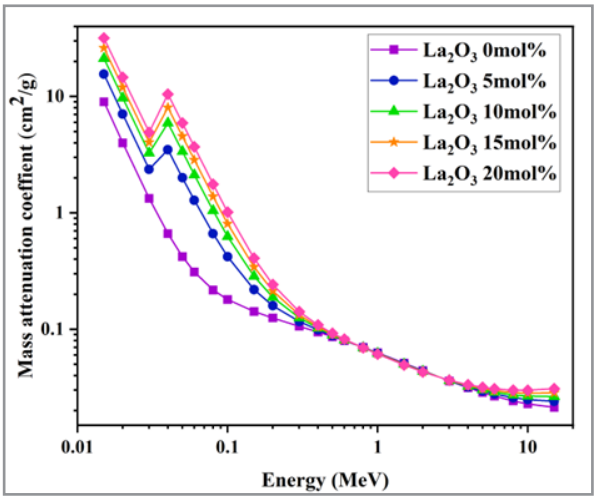

Figure 8: The MAC of glass samples.

The effective atomic number (Zeff) of glass samples can depicted results in Fig. 9. The Zeff values slightly increased with La3+ ions increase. It is observed that Zeff of glass samples initially increases with rising photon energy up to 0.04 MeV, showing abrupt jupms between 0.03-0.04 MeV. These sudden shifts are attributed to the K-edge absorption of La3+ ions at approximately 38.9 keV. Within the energy range of 0.015–0.02 MeV, Zeff values for the glass samples remain relatively constant and independent of photon energy. From 0.06 MeV to 0.2 MeV, a significant decrease in Zeff is noted as incident photon energy increases, due to the inverse relationship between the photoelectric absorption cross-section and photon energy. In energy regions dominated by Compton scattering and pair production, the addition of La3+ ions cause minimal change in the electron denstiy (Neff) cause of their high photon transmission attenuation. The behavior Neff closely follows that the Zeff [24, 25].

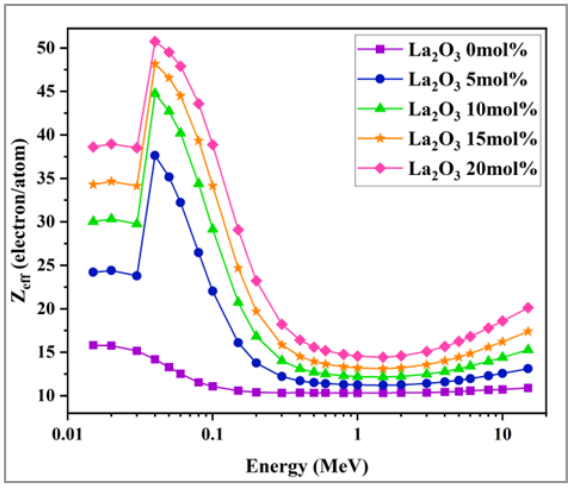

Figure 9: The Zeff of Glass Samples with XCOM Program.

The electron density (Neff) of glass samples can be depicted in Fig. 10. The Neff values for gamma ray energies and the La3+ ions exhibited similar curves to those of Zeff and MAC. A significantly enhanced value of Neff this reflects a higher probability of photon-matter interanction occurring in glass composition.

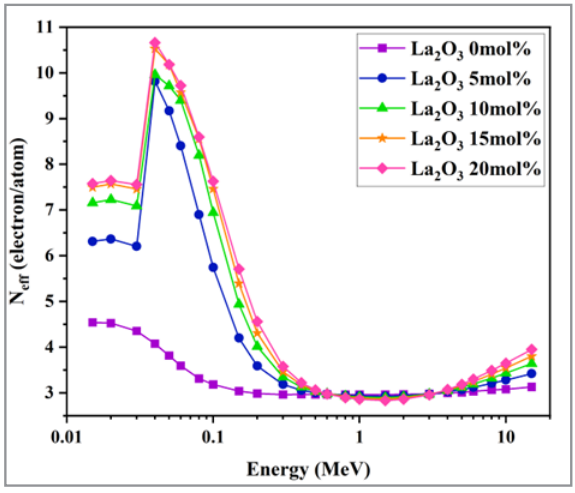

Figure 10: The Neff of Glass Samples with XCOM Program

The X-ray radiation shielding performance in context of half value layer (HVL), ten value layer (TVL) and mean free path (MFP) is closely correlated with key parameters uses in radiation dose calculations, including shielding materials properties, thickness and photon energy are show in Table.1

Table 1: Radiation Shielding Parameter Data

Glass sample	Energy(kVp)	MAC (cm2/g)	HVL (cm)	TVL (cm)	MFP (cm)
La 0mol%	50	1.973±0.033	0.132±0.004	0.439±0.002	0.191±0.001
	60	1.854±0.015	0.141±0.003	0.468±0.003	0.203±0.002
	70	1.195±0.011	0.218±0.003	0.726±0.005	0.315±0.003
	80	0.911±0.007	0.286±0.002	0.951±0.003	0.413±0.002
	90	0.633±0.006	0.412±0.003	1.370±0.002	0.595±0.003
	100	0.517±0.004	0.504±0.001	1.676±0.003	0.728±0.001
	110	0.314±0.002	0.831±0.002	2.760±0.001	1.199±0.003
	120	0.152±0.008	1.714±0.001	5.695±0.001	2.474±0.004
La 5mol%	50	5.700±0.065	0.044±0.002	0.146±0.003	0.063±0.003
	60	5.056±0.021	0.050±0.002	0.165±0.005	0.072±0.002
	70	3.772±0.006	0.066±0.001	0.221±0.001	0.096±0.003
	80	3.306±0.004	0.076±0.003	0.252±0.002	0.109±0.003
	90	3.179±0.003	0.079±0.003	0.262±0.003	0.114±0.007
	100	2.047±0.004	0.123±0.002	0.407±0.003	0.177±0.002
	110	1.941±0.002	0.129±0.001	0.429±0.001	0.186±0.001
	120	1.816±0.002	0.138±0.001	0.459±0.001	0.199±0.004
La 10mol%	50	6.329±0.045	0.039±0.006	0.130±0.007	0.057±0.002
	60	5.845±0.013	0.042±0.002	0.141±0.002	0.061±0.001
	70	4.272±0.005	0.058±0.001	0.193±0.003	0.084±0.003
	80	3.702±0.004	0.067±0.003	0.223±0.003	0.097±0.003
	90	3.544±0.003	0.070±0.003	0.232±0.002	0.101±0.002
	100	3.082±0.003	0.080±0.002	0.267±0.001	0.116±0.001
	110	2.714±0.002	0.091±0.003	0.304±0.001	0.132±0.002
	120	2.204±0.003	0.113±0.001	0.374±0.000	0.162±0.001
La 15mol%	50	7.222±0.032	0.034±0.002	0.113±0.004	0.049±0.003
	60	6.376±0.014	0.038±0.001	0.128±0.003	0.056±0.002
	70	4.662±0.008	0.053±0.003	0.175±0.002	0.076±0.001
	80	4.231±0.005	0.058±0.002	0.193±0.001	0.084±0.002
	90	3.896±0.004	0.063±0.002	0.209±0.002	0.091±0.001
	100	3.750±0.003	0.065±0.004	0.217±0.006	0.094±0.002
	110	2.918±0.003	0.084±0.001	0.279±0.003	0.121±0.001
	120	2.517±0.001	0.097±0.001	0.324±0.001	0.141±0.000
La 20mol%	50	8.147±0.039	0.030±0.003	0.098±0.001	0.043±0.001
	60	6.862±0.012	0.035±0.003	0.117±0.002	0.051±0.002
	70	4.933±0.011	0.049±0.002	0.162±0.003	0.071±0.003
	80	4.507±0.009	0.054±0.005	0.178±0.003	0.077±0.002
	90	4.181±0.006	0.058±0.001	0.192±0.004	0.083±0.001
	100	4.035±0.004	0.060±0.002	0.199±0.002	0.086±0.002
	110	3.107±0.002	0.078±0.002	0.258±0.001	0.112±0.001
	120	2.893±0.001	0.083±0.001	0.277±0.000	0.120±0.001

Conclusion

Lead-free radiation shielding materials are advantageous for human health, environmental, particularly for manufacturer process, due to their toxicity. In this research focused on lanthanum doped glasses as a potential alternative shielding materials in glass samples system in the formula (60-x) P2O5: 15Na2O: 5ZnO: 10Al2O3: 10CaO: xLa2O3 where x is 0, 5, 10, 15 and 20 mol%, respectively, and has been synthesized by melt-quenching, was investigated. It found that radiation shielding in photon energy with x-ray and gamma ray of glass samples increase as

the concentration La3+ ions increase. The HVL in x-ray regions is better than standard radiation shielding. The theoretical values, XCOM programs, there is a tendency for radiation shielding values to align in the same direction. This work suggests that La3+ ions are good substitute for lead-free radiation shielding, exhibiting non-toxic effects on the environment, and can be considered as new alternative candidate to lead free advanced radiation shielding materials moving forward.

Acknowledgment

This project is funded by National Research Council of Thailand (NRCT) and Chiang Mai University (Contract number N42A670708). The authors would like to thank CEGM, Nakhon Pathom Rajabhat University for supporting the technique of glass preparation and instruments and thanks to Chiang Mai University for supporting the work. O. Ornketphon has received TA/RA scholarship from The Graduate School, Chiang Mai University for supporting glass preparation, facilities, and funding.

Reference

1. Al-Buriahi, M. S. (2023). Radiation shielding performance of a borate-based glass system doped with bismuth oxide. Radiation Physics and Chemistry, 207, 110875. https://doi.org/10.1016/j.radphyschem.2023.110875
2. Al-Buriahi, M. S., Alrowaili, Z. A., Alsufyani, S. J., Olarinoye, I. O., Alharbi, A. N., Sriwunkum, C., & Kebaili, I. (2022). The role of PbF_2 on the gamma-ray photon, charged particles, and neutron shielding prowess of novel lead fluoro bismuth borate glasses. Journal of Materials Science: Materials in Electronics, 33(3), 1123–1139. https://doi.org/10.1007/s10854-021-07382-4
3. Kaewjaeng, S., Kothan, S., Chaiphaksa, W., Chanthima, N., Rajaramakrishna, R., Kim, H. J., & Kaewkhao, J. (2019). High transparency La_2O_3–CaO–B_2O_3–SiO_2 glass for diagnostic X-ray shielding material application. Radiation Physics and Chemistry, 160, 41–47. https://doi.org/10.1016/j.radphyschem.2019.03.018
4. Kaewjaeng, S., Boonpa, W., Khrongchaiyaphum, F., Kothan, S., Kim, H. J., Intachai, N., Rajaramakrishna, R., Kiatwattanacharoen, S., & Kaewkhao, J. (2021). Influence of trivalent praseodymium ion on SiO_2–B_2O_3–Al_2O_3–BaO–CaO–Sb_2O_3–Na_2O–Pr_2O_3 glasses for X-ray shielding and luminescence materials. Radiation Physics and Chemistry, 184, 109467. https://doi.org/10.1016/j.radphyschem.2021.109467
5. Mutuwong, C., Nutaro, T., & Saiz, A. (2018). Comparative studies of gamma-ray shielding properties of the PbO–BaO–B_2O_3 glass system by using FLUKA code, XCOM program, and accessible experimental data. Journal of Physics: Conference Series, 1144, 012130. https://doi.org/10.1088/1742-6596/1144/1/012130
6. Kaur, D., Reddy, M. S., & Pandey, O. P. (2021). Synthesis, characterization, drug loading, and in-vitro bioactivity studies of rice husk-derived SiO_2–P_2O_5–MgO–CaO–SrO bioactive glasses. Journal of Drug Delivery Science and Technology, 61, 102154. https://doi.org/10.1016/j.jddst.2020.102154
7. Meejitpaisan, P., Doddoji, R., Kothan, S., Jayasankar, C. K., & Kaewkhao, J. (2021b). Visible to infrared emission from (Eu^{3+}/Nd^{3+}): B_2O_3 + AlF_3 + NaF + CaF_2 glasses for luminescent solar converters. Optics & Laser Technology, 141, 107170. https://doi.org/10.1016/j.optlastec.2021.107170
8. Meejitpaisan, P., Doddoji, R., Kothan, S., Jayasankar, C. K., & Kaewkhao, J. (2021a). Intense red emission via energy transfer from (Ce^{3+}/Eu^{3+}): P_2O_5 + NaF + CaF_2 + AlF_3 glasses for warm light sources. Ceramics International, 47(2), 1962–1969. https://doi.org/10.1016/j.ceramint.2020.09.026
9. Kaewjaeng, S., Kothan, S., Jumpee, C., Kiatwattanacharoen, S., Wongdamnern, N., Kedkaew, C., Sareein, T., & Kaewkhao, J. (2021). Direct and quantitative study of Gd^{3+} doped Na_2O–Al_2O_3–SiO_2–B_2O_3–CeF_3 glass samples for radiation interaction parameters. Integrated Ferroelectrics, 223(1), 29–37. https://doi.org/10.1080/10584587.2021.1964283
10. Council, J. L., Blasco, E., Moreno, A., Marín, N., & Feliu, C. (2020). Sinter-crystallisation kinetics of a SiO–AlO–CaO–MgO–SrO glass-ceramic glaze. Journal of Non-Crystalline Solids, 532, 119900. https://doi.org/10.1016/j.jnoncrysol.2020.119900
11. Jarucha, N., Ruangtaweep, Y., Meejitpaisan, P., Nawarat, P., Kanthang, P., Wongdamnern, N., Limsuwan, P., Kim, H. J., Kaewkhao, J., & Sareein, T. (2023). Effect of Eu_2O_3 concentrations doped Li–Na–K borate glasses on luminescence properties for red emission material. Integrated Ferroelectrics, 238(1), 309–316. https://doi.org/10.1080/10584587.2023.2234578
12. Meejitpaisan, P., Kaewjaeng, S., Ruangthaweep, Y., Sangwarantee, N., & Kaewkhao, J. (2021). White light emission of gadolinium calcium phosphate oxide and oxyfluoride glasses doped with Dy^{3+}. Materials Today: Proceedings, 43, 2574–2587. https://doi.org/10.1016/j.matpr.2020.04.619
13. Kaewjaeng, S., Wantana, N., Kothan, S., Rajaramakrishna, R., Kim, H. J., Limsuwan, P., & Kaewkhao, J. (2021). Effect of Gd_2O_3 on the radiation shielding, physical, optical, and luminescence behaviors of Gd_2O_3–La_2O_3–ZnO–B_2O_3–Dy_2O_3 glasses. Radiation Physics and Chemistry, 185, 109500. https://doi.org/10.1016/j.radphyschem.2021.109500
14. National Council on Radiation Protection and Measurements. (n.d.). By authority of the United States of America: Legally binding document.
15. Almatari, M. (n.d.). Energy absorption and exposure buildup factors for some bioactive glass samples: Penetration depth, photon energy, and atomic number dependence. Journal of Optoelectronics and Biomedical Materials, 9(2).
16. Alsaif, N. A. M., Elmahroug, Y., Alotaibi, B. M., Alyousef, H. A., Rekik, N., Hussein, A. W. M. A., Chand, R., & Farooq, U. (2021). Calculating photon buildup factors in determining the γ-ray shielding effectiveness of some materials susceptible to be used for the conception of neutrons and γ-ray shielding. Journal of Materials Research and Technology, 11, 769–784. https://doi.org/10.1016/j.jmrt.2021.01.052
17. Al-Saleh, W. M., Dahi, M. R. H., Sayyed, M. I., Almutairi, H. M., Saleh, I. H., & Elsafi, M. (2023). Comprehensive Karpuz, N. (2023). Radiation shielding properties of glass composition. Journal of Radiation Research and Applied Sciences, 16(4), 100689. https://doi.org/10.1016/j.jrras.2023.100689
18. Kuluöztürk, Z. N. (2023). Gamma-ray shielding properties of soda-lime glass and glass ceramic: An experimental and Monte Carlo simulation study. Radiation Physics and Chemistry, 212, 111172. https://doi.org/10.1016/j.radphyschem.2023.111172
19. Li, D., Guo, Y., Wang, G., & Ge, L. (2022). Calculation

and study on the exposure buildup factor of type 316 stainless steel. OALib, 9(5), 1–12. https://doi.org/10.4236/oalib.1108679

20. Mahmoud, K. A., Tashlykov, O. L., Almuqrin, A. H., Sayyed, M. I., & Vlasova, S. G. (2022). Assessment of mechanical and radiation shielding capacity for a ternary CdO–BaO–B_2O_3 glass system: A comprehensive experimental, Monte Carlo simulation, and theoretical study. Progress in Nuclear Energy, 146, 104169. https://doi.org/10.1016/j.pnucene.2022.104169
21. Olarinoye, I. O., Odiaga, R. I., & Paul, S. (2019). EXABCal: A program for calculating photon exposure and energy absorption buildup factors. Heliyon, 5(7), e02017. https://doi.org/10.1016/j.heliyon.2019.e02017
22. Salehi, D., Sardari, D., & Jozani, M. S. (2015). A study of energy absorption and exposure buildup factors in natural uranium. Advances in Materials Research, 4(1), 23–30. https://doi.org/10.12989/amr.2015.4.1.23
23. Sayyed, M. I., & Elhouichet, H. (2017). Variation of energy absorption and exposure buildup factors with incident photon energy and penetration depth for boro-tellurite (B_2O_3–TeO_2) glasses. Radiation Physics and Chemistry, 130, 335–342. https://doi.org/10.1016/j.radphyschem.2016.09.019
24. Subedi, B., Paudel, J., & Lamichhane, T. R. (2023). Gamma-ray, fast neutron, and ion shielding characteristics of low-density and high-entropy Mg–Al–Ti–V–Cr–Fe–Zr–Nb alloy systems using Phy-X/PSD and SRIM programs. Heliyon, 9(7), e17725. https://doi.org/10.1016/j.heliyon.2023.e17725